Available online at www.sciencedirect.com
SCIENCE DIRECT®
Trans. Nonferrous Met. Soc. China 16(2006) 259−266
Transactions of Nonferrous Metals Society of China
www.csu.edu.cn/ysxb/

Fabrication and characterization of hydroxyapatite/Al_2O_3 biocomposite coating on titanium

WU Zhen-jun(吴振军)[1], HE Li-ping(何莉萍)[2], CHEN Zong-zhang(陈宗璋)[1]

1. College of Chemistry and Chemical Engineering, Hunan University, Changsha 410082, China;
2. College of Mechanical and Automotive Engineering, Hunan University, Changsha 410082, China

Received 2 June 2005; accepted 2 August 2005

Abstract: A novel biocomposite coating of hydroxyapatite/Al_2O_3 was fabricated on titanium using a multi-step technique including physical vapor deposition(PVD), anodization, electrodeposition and hydrothermal treatment. Anodic Al_2O_3 layer with micrometric pore diameter was formed by anodization of the PVD-deposited aluminum film on titanium and subsequent removal of part barrier Al_2O_3 layer. Hydroxyapatite coating was then electrodeposited onto the as-synthesized anodic Al_2O_3 on titanium. A hydrothermal process was finally applied to the fabricated biocomposite coating on titanium in alkaline medium. Scanning electron microscopy(SEM), energy dispersive spectrometry(EDS) and X-ray diffractometry(XRD) were employed to investigate the morphologies and compositions of the pre- and post-hydrothermally treated hydroxyapatite/Al_2O_3 biocomposite coatings. The results show that micrometric plate-like Ca-deficient hydroxyapatite (CDHA) coatings are directly electrodeposited onto anodic Al_2O_3 at constant current densities ranging from 1.2 to 2.0 mA/cm^2 using NaH_2PO_4 as the phosphorous source. After hydrothermal treatment, the micrometric plate-like CDHA coating electrodeposited at 2.0 mA/cm^2 is converted into nano-network Ca-rich hydroxyapatite (CRHA) one and the adhesion strength is improved from 9.5 MPa to 21.3 MPa. A mechanism of dissolution-recrystallization was also proposed for the formation of CRHA.

Key words: anodic Al_2O_3; hydroxyapatite; biocomposite coating; medical metals; PVD; electrodeposition; hydrothermal treatment

1 Introduction

Currently, many synthetic materials, such as medical metals (titanium and its alloys), Bioglass®, CaP bioceramics, alumina, and some biodegradable polymers and so on, have been developed for hard tissue repair and replacement[1,2]. Among these available systems, titanium and its alloys coated with hydroxyapatite(HA), a kind of CaP bioceramic with formula of $Ca_{10}(PO_4)_6(OH)_2$ which serves as the main inorganic composition of human bone[3], have attracted much attention due to the simultaneous achievements of good mechanical properties and superior biocompatibility[4, 5]. So far, some methods, including plasma spray[6], laser ablation[7], sol-gel process[8], biomimetic growth [9], electrocrystallization[10], and electrophoretic deposition[11], have been applied to the fabrication of HA coatings on medical metals. However, the HA-coated medical metals fabricated by these methods still have some disadvantages including the release of toxic elements from metal substrate, thermal expansion mismatch of HA coating and metal substrate, and compositional diversity of the outer coating because of the non-total covering and high temperature contained in the fabrication procedure inherently or subsequently [12, 13].

To solve the problems mentioned above, several recent studies have focused on the introduction of intermediate layers, as examples of microarc TiO_2 and anodic Al_2O_3, between bioactive HA coating and metal substrate and obtained some helpful results[14−17]. Especially, an in situ CaP(aggregate)/Al_2O_3 composite coating with as-designed “T” shape effect has been successfully fabricated on titanium in our previous work [16,17]. But to achieve long-term reliable biocompatibility, HA outer layer is preferable. Hereinafter, a modified multi-step technique combining physical vapor deposition(PVD), anodization, electrodeposition, and hydrothermal treatment is

Foundation item: Project(50472031) supported by the National Natural Science Foundation of China
Corresponding author: CHEN Zong-zhang; Tel: +86-731-8822276; E-mail: wooawt@yahoo.com.cn

employed to fabricate a novel HA/Al_2O_3 biocomposite coating on titanium. The morphologies and compositions of as-fabricated biocomposite coatings were investigated by scanning electron microscopy(SEM), energy dispersive spectrometry(EDS), and X-ray diffractometry (XRD). A mechanism for the formation of Ca-rich HA (CRHA) layer during hydrothermal treatment was also proposed.

2 Experimental

2.1 Fabrication process

The raw materials and chemicals used in the present work are as follows.

Commercially pure titanium discs (Ti, d18 mm×1 mm, >95%, China), PVD Al target (>99.99%, UK), $Na_3PO_4 \cdot 12H_2O$ (analytic reagent, ⩾ 97%, China), $Ca(NO_3)_2 \cdot 4H_2O$ (analytic reagent, ⩾ 99%, China), $NaH_2PO_4 \cdot 2H_2O$ (analytic reagent, ⩾ 99%, China), NaOH (analytic reagent, ⩾96%, China).

The procedure for fabricating hydroxyapatite/Al_2O_3 biocomposite coating on titanium is schematically shown in Fig.1. The processes including PVD, anodization, electrodeposition, and hydrothermal treatment are detailed as below.

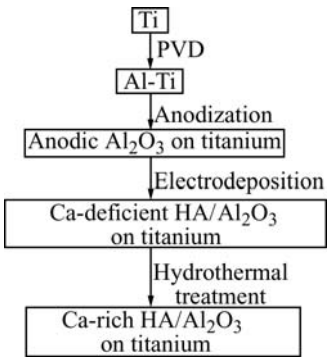

Fig.1 Fabrication procedure of HA/Al_2O_3 biocomposite coating on titanium

1) Deposition of Al film on titanium by PVD

Commercially pure titanium was cut into small discs with a dimension of 18 mm diameter and 1 mm thickness. The titanium discs were mechanically ground and polished, ultrasonically washed with acetone and deionized water. After pre-treatment, titanium discs were then used as substrates subjected to PVD. The deposition of Al film was carried out by a magnetron sputtering ion plating system (TEER, UK) using highly pure Al (>99.99%) as target under the condition of −100 V bias voltage, 5.0 A aluminum target current, and 60 min duration at a pressure of 2.66×10^{-4} Pa. Pure aluminum film with a thickness of approximately 2.5 μm finally formed on titanium disc.

2) Anodization of Al film on titanium

The PVD-deposited Al film on titanium was ultrasonic-washed in acetone for 20 min to clean its surface. And then the pre-treated Al film was anodized potentiostatically in 100 g/L Na_3PO_4 solution at 80 V and 15 ℃ for 30 min using a two-electrode electrolytic system, in which the titanium disc deposited with Al film acted as anode (working electrode) and a stainless steel plate as cathode (counter electrode). The distance between anode and cathode was fixed at 3.5 cm. To reduce the resistance of anodic Al_2O_3 and prompt the soakage of electrolyte during electrodeposition, the anodized specimens were immersed in a 5% phosphoric acid solution at 30 ℃ for 40 min. After this process, the barrier layer of anodic Al_2O_3 became thinner, and accordingly the pores were widened.

3) Electrodeposition

The electrolyte for electrodeposition was an aqueous solution containing 0.08 mol/L $Ca(NO_3)_2$ and 0.04 mol/L NaH_2PO_4. The pH value of electrolyte was adjusted to 5-6 by 0.1 mol/L NaOH solution. Electrodeposition was performed at constant current densities ranging from 0.25 to 2.0 mA/cm^2 and 23 ℃ for 15 min with mild magnetic stirring. The cathode (working electrode) was titanium disc covered with anodic Al_2O_3 and the anode (counter electrode) was a platinum plate. The distance between anode and cathode was 3.0 cm.

4) Hydrothermal treatment

The composite coatings formed on titanium were hydrothermally treated at 150, 170, 190 ℃ with a pressure of 1.25 MPa for 4 h in an autoclave. The hydrothermal medium was an alkaline solution of ammonia (25%−28% in water)-water (1:80 in volume ratio). The hydrothermally treated specimens were finally dried at 100 ℃ for 1 h in a resistance furnace.

2.2 Characterization and analysis

The morphologies of anodic Al_2O_3 with widened pores, the electrodeposited coatings, and the hydrothermally treated composite coatings were characterized by scanning electron microscopy (SEM, JEOL/JSM-5600) at an acceleration voltage of 20 kV. The element types and their atomic percentages of the pre- and post-hydrothermally treated composite coatings were determined by energy dispersive spectrometry (EDS) attached to SEM. X-ray diffractometry(XRD, Siemens D5000) was conducted to analyze phases of the obtained biocomposite coatings on titanium using CuK_α radiation at a voltage of 35 kV with a current of 30 mA and a scanning rate of 0.04 (°)/s.

The composite coating electrodeposited at 2.0 mA/cm^2 was used as the sample subjected to tensile test and its adhesive strength was determined before and after hydrothermal treatment at a motion rate of 0.02 mm/s by

an electronic versatile materials testing machine (CMT-7105, China). The binder was a mixture of epoxy resin and polyamide resin (1:1).

3 Results and discussion

3.1 Formation of anodic Al_2O_3 with big pores on titanium

Fig.2 shows the surface morphology of PVD-deposited Al film on titanium. Compared with the one obtained at 4.5 A target current in Ref.[16], no obvious protrudent aggregation is observed in Fig.2, which indicates a good amalgamation of aluminum crystal during PVD at 5 A. It is thought that even surface of Al film is beneficial for the formation of anodic Al_2O_3 with uniform pores[18]. Therefore, a PVD target current higher than 5 A is preferable for the uniform deposition of HA coating.

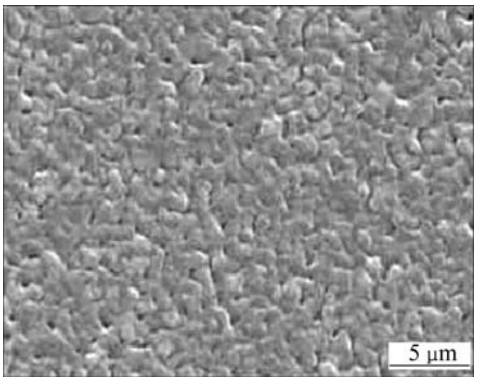

Fig.2 Surface morphology of PVD-deposited Al film on titanium

Fig.3 exhibits anodic behavior of PVD-deposited Al film on titanium. It is a typical curve of aluminum anodization at constant cell voltage, which consists of three continuous phases, namely, a quick drop of current density, then the increase of current density, and finally the stabilization of current density, indicating the fast formation of barrier Al_2O_3 layer, the initial growth of porous Al_2O_3 layer, and the further development of porous Al_2O_3 layer, respectively[19]. There is no obvious decrease of current density once again in the curve as shown in Fig.3 after the formation stage of porous Al_2O_3 layer, suggesting that the anodization of PVD-deposited Al film on titanium is incomplete. This case also could be elucidated from the fact that compact anodic TiO_2 layer with higher resistance would lead to an obvious decrease of current density if anodization reaches the titanium substrate[20].

It has been proved that there were only fine pores with diameter less than 300 nm formed on pure aluminum using Na_3PO_4 electrolyte at tens of cell voltages[21]. To prompt a good soakage of solution and obtain uniform HA coating during electrodeposition, anodic Al_2O_3 layer on titanium with uniform big pores and better conductivity is needed. For this purpose, it is considered that chemical dissolution of anodic Al_2O_3 in diluted H_3PO_4 is feasible. When immersed in diluted H_3PO_4, the bottom and the wall of pores can be chemically dissolved and thus the barrier Al_2O_3 layer becomes thinner, and meanwhile, the pores of anodic Al_2O_3 layer were widened[22]. This process was applied to the anodic Al_2O_3 on titanium in the present work. Uniform pores with diameter approximately 1 μm, can be clearly observed from the SEM micrograph of the prepared anodic Al_2O_3 on titanium as shown in Fig.4.

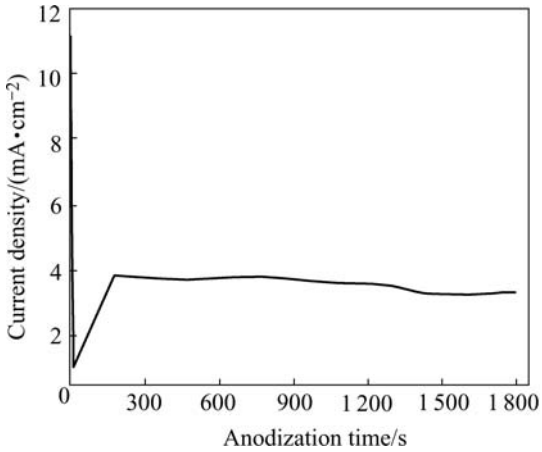

Fig.3 Anodic behavior curve of PVD-deposited Al film on titanium at constant voltage of 80 V in Na_3PO_4 solution

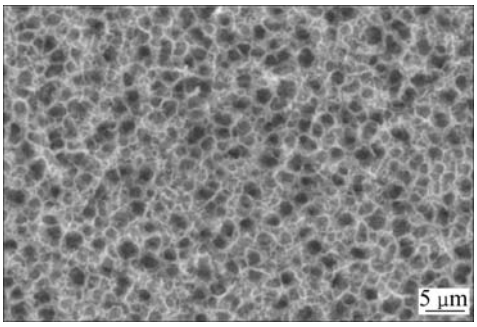

Fig.4 Surface morphology of porous anodic Al_2O_3 after immersed in 5% phosphoric acid solution at 30 ℃ for 40 min

3.2 Effect of current density on morphologies and compositions of electrodeposits

The electrodeposition of the ions containing calcium and phosphorous onto porous surface of anodic Al_2O_3 was conducted at constant current mode. $Ca(NO_3)_2$ and NaH_2PO_4 served as the calcium source and the phosphorous source, respectively. Fig.5 shows the electrodeposition rate, which is expressed as the electrodeposited mass of one milliampere within one minute and denoted as v_C, at different current densities as the anodic Al_2O_3 area on titanium for electrodeposition is

kept at 2.0 cm^2. v_C increases firstly with the current density and reaches a maximum value at approximately 1.2 mA/cm^2, and then decreases at higher current density accompanied by the obvious release of H_2. Therefore, the appropriate current density should be set at 1−2 mA/cm^2 to obtain enough electrodeposits and to avoid too much H_2 release during electrodeposition.

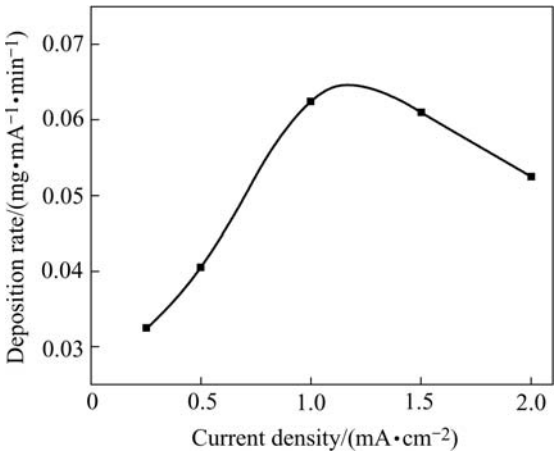

Fig.5 Variation of electrodeposition rate with current density at identical substrate area (2.0 cm^2)

Fig.6 shows the surface morphologies of electrodeposits formed at different current densities. The electrodeposited coatings are mainly constructed with plate-like crystals with 10−25 μm length and 2−5 μm width growing away from the substrates. The images suggest that the higher the current density is, the bigger and denser the electrodeposited crystals are.

According to the XRD patterns shown in Fig.7, the electrodeposits prepared at different current densities are hydroxyapatite(HA) coatings. Besides the diffraction peaks of titanium substrate and anodic Al_2O_3, some characteristic peaks of HA can also be observed at the angles of 26° and 30°−34°, which corresponding to the (002), (211), (112), and (300) diffractions. It is clear that there is an orientation growth of (002) plane in HA, which consists with the observation by others when electrodepositing bioactive coatings[23]. It is also found from Fig.7 that the diffraction peaks of (211), (112), and (300) planes are intensified while the diffraction peak of (002) is weakened with the increase of current density. This indicates that the structure of electrodeposited crystal is more similar to that of the standard HA at higher current density, which can also be identified according to mole ratios of Ca to P closer to 1.67 as shown in Table 1.

Table 1 also shows that the mole ratios of Ca to P of the direct electrodeposits on anodic Al_2O_3 are less than 1.67 (the mole ratios of Ca to P of stoichiometric HA). This may be due to the incorporation of HPO_4 groups into the lattice of apatite crystal and a resulting layer of

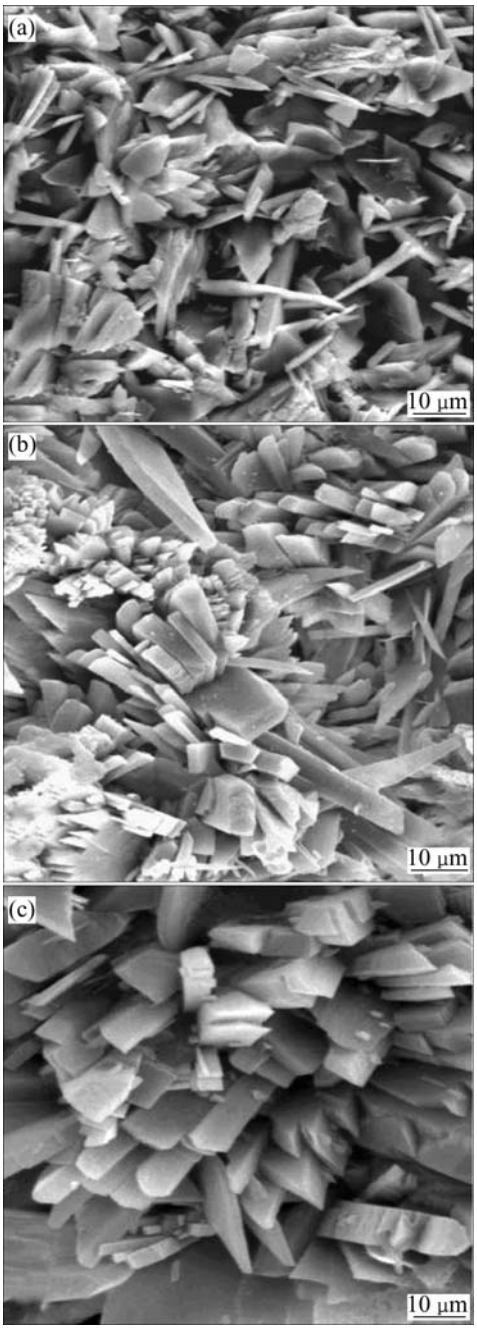

Fig.6 Surface morphologies of coatings electrodepsited at different current densities: (a) 1.2 mA/cm^2; (b) 1.7 mA/cm^2; (c) 2.0 mA/cm^2

Table 1 Mole ratios of Ca to P of coatings electrodeposited on anodic Al_2O_3 at different current densities

Current density/ ($mA\cdot cm^{-2}$)	Electrodeposited coatings	Standard HA
1.2	1.55	
1.7	1.59	1.67
2.0	1.62	

Ca-deficient HA (CDHA) with molecular formula of $Ca_{10-x}(HPO_4)_x(PO_4)_{6-x}(OH)_{2-x}$ $(0\leqslant x\leqslant 1)$ formed[24]. The content of HPO_4 groups, denoted by the value of x,

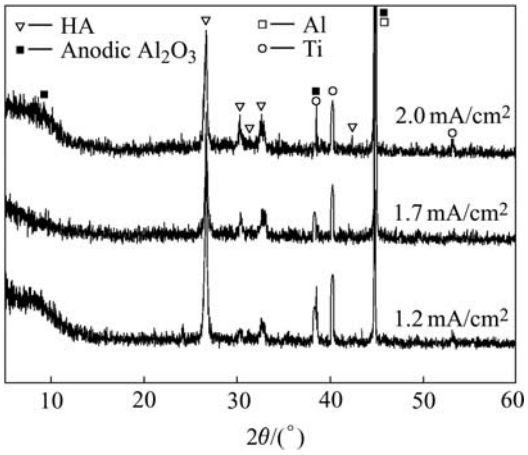

Fig.7 XRD patterns of coatings electrodeposited on anodic Al_2O_3-Ti at different current densities

can be calculated from the formula as

$$\frac{10-x}{x+(6-x)}=R_{Ca/P} \quad (1)$$

where $R_{Ca/P}$ is the mole ratio of Ca to P. It has been reported that the structural characterization of CDHA is similar to that of standard HA[25], therefore, the diffraction peaks of the obtained CDHA coating, as shown in Fig.7, are in a good agreement with those of stoichiometric HA. In addition, no titanium element is detected by EDS due to the shielding effect of aluminum, which consists with the EDS result obtained by our previous work[17] and also identifies the incomplete anodization of PVD-deposited Al film on titanium substrate just as concluded from Fig.3.

It is interesting that the direct deposition of HA, although not stoichiometric one, is realized in the present work using NaH_2PO_4 as phosphorus source and NaOH as buffering reagent. Differently, $NH_4H_2PO_4$ is often used as the phosphorus source to electrodeposit bioceramic coatings on medical metals and non-HA products, such as brushite and other CaP phases, have been obtained[26]. It is generally accepted that the formation of non-HA deposits should be due to the lack of OH^- ions around the cathode[27]. Although high current density can increase the concentration of OH^- ions surrounding cathode by consuming more H^+ ions or producing OH^- ions directly[28] through the cathodic reactions as

$$2H^++2e=H_2\uparrow \quad (2)$$

$$H_2O+2e=2OH^-+H_2\uparrow \quad (3)$$

$$O_2(\text{dissolved})+2H_2O+4e=4OH^- \quad (4)$$

However, there exist unavoidable disadvantages, such as the formation of many spiracles in the coatings and the adhesive strength decrease of deposits due to the release of too much H_2 gas. Thus, high current density is improper for the fabrication of bioceramic coatings with good adhesion.

When using $NH_4H_2PO_4$ as phosphorus source, another cathodic reaction occurs

$$NH_4^++OH^-=NH_3\uparrow+H_2O \quad (5)$$

Reaction(5) would be accelerated because of the NH_3 gas evolution during the continuous motion of NH_4^+ ions to cathode under the driving of potential difference. Furthermore, the continuous releasing H_2 also can act as carrier to take the generated NH_3 away from cathode. Hence, additional OH^- ions consumption caused by reaction(5) could be avoided through the substitution of Na^+ for NH_4^+ in the present work. Therefore, the produced OH^- ions may be enough for the formation of HA. This indicates that the electrolyte type could be one of key factors for the direct electrodeposition of HA.

3.3 Effect of hydrothermal temperature on compositions and morphologies of composite coatings

Fig.8 shows the XRD patterns of the electrodeposited CDHA with 2.0 mA/cm^2 after hydrothermal treatment at different temperatures. Compared with the directly electrodeposited coating(EC), the hydrothermally treated ones are still composed of HA according to their XRD patterns. With the increase of hydrothermal temperature, the diffraction peaks corresponding to (211), (112), and (300) become higher than the one to (002), indicating that the hydrothermal treatment leads to higher crystallinity of the electrodeposited coatings.

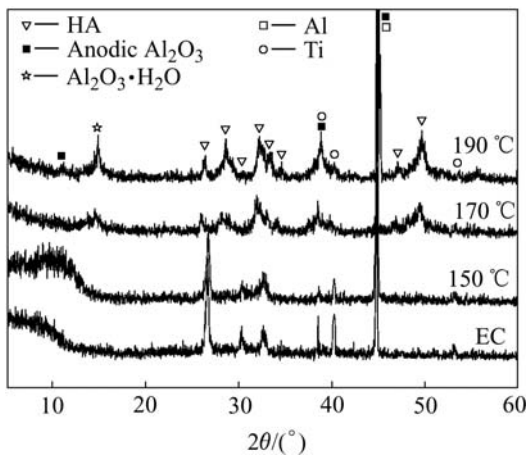

Fig.8 XRD patterns of electrodeposited coating (EC, 2.0 mA/cm^2) on anodic Al_2O_3-Ti after hydrothermal treatment at different temperatures

The SEM images of the hydrothermally treated coatings at different temperatures are given in Fig.9, showing that the coatings become more uniform with the increase of hydrothermal temperature. The micrometric outer plate-like HA coating (Fig.6(c)) is transformed into

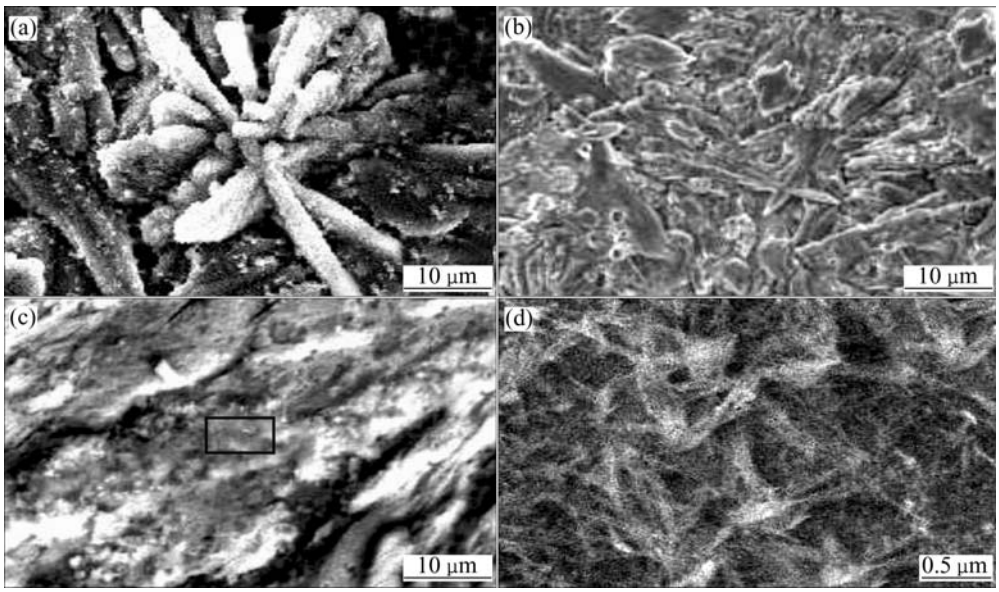

Fig.9 SEM images of electrodeposited coating (EC, 2.0 mA/cm^2) after hydrothermal treatment at different temperatures: (a) 150 ℃, (b) 170 ℃, (c) 190 ℃; (d) Magnified photo of framed area in (c)

nanometric network-like (Fig.9(d)) one at 190 ℃. It is expected that this network-like structure textured with nanowires could stimulate the in-growth of new-born bone to achieve a "T" shape effect as designed by our previous work[16], which can also enhance the adhesive strength between bioceramic coating and substrate.

The EDS results in Table 2 show that the electrodeposited CDHA is converted into Ca-rich hydroxyapatite(CRHA) with mole ratio of Ca to P higher than 1.67 after being hydrothermally treated at 190 ℃ for 4 h.

Table 2 Experimental and theoretical Ca/P atomic ratios of the coatings electrodeposited on anodic Al_2O_3 with different current densities after hydrothermal treatment at 190 ℃

Current density/ (mA·cm^{-2})	x(CDHA)	$R_{ca/P}$	
		Exp.	Cal.
1.2	0.70	1.96	2.32
1.7	0.46	2.01	2.38
2.0	0.28	2.29	2.43

It has been proposed that a mechanism, including the chemical dissolution of CaP phases, then static adsorption of Ca^{2+}, and final induction of HA, may contribute to the formation of CRHA in synthetic fluid [29]. Thereinafter, a mechanism similar to the one in synthetic fluid for the formation of CRHA outer layer in the present biocomposite coating is outlined.

During hydrothermal treatment, the alkaline ammonia could be ionized to form OH^- as

$$NH_3{\cdot}H_2O = NH_4^+ + OH^- \tag{6}$$

The electrodeposited CDHA would react with OH^- ions and then be converted to stoichiometric HA based on the following reactions:

$$Ca_{10-x}(HPO_4)_x(PO_4)_{6-x}(OH)_{2-x} + 6OH^- = (4-x)Ca(OH)_2 + 2Ca_3(PO_4)_2 + 2\,PO_4^{3-} + xH_2O \tag{7}$$

$$Ca(OH)_2 + 3Ca_3(PO_4)_2 = Ca_{10}(PO_4)_6(OH)_2 \tag{8}$$

Because reaction(8) could not consume all $Ca(OH)_2$, which is produced more than $Ca_3(PO_4)_2$ according to the chemical equilibrium of reaction(7), the remaining $Ca(OH)_2$ would be contained in the stoichiometric HA newly formed through reaction(8) since $Ca(OH)_2$ is a kind of relatively stable calcium precipitate in alkaline medium. While the resultant PO_4^{3-} from reaction(7) may form ammonium phosphate salt and dissolve in the hydrothermal medium. According to reaction(7), the theoretical mole ratios of Ca to P of CRHA, shown as $R^{\oplus}_{Ca/P}$, can be calculated from the formula as below:

$$\frac{(4-x)+2\times 3}{2\times 2} = R^{\oplus}_{Ca/P} \tag{9}$$

Based on Eqn.(1), x value of the electrodeposited CDHA with different current densities can be obtained. The corresponding theoretical mole ratios of Ca to P of CRHA are then calculated from the obtained x values according to formula (9) and displayed in Table 2. Although the solubility is very low, there is still some dissolved $Ca(OH)_2$ entering into hydrothermal medium since these experimental mole ratios of Ca to P are less than the theoretical ones as shown in Table 2.

The high dispersity of the resulting $Ca(OH)_2$ precipitate contained in stoichiometric HA or the overlap of diffraction peaks may lead to no discovery of $Ca(OH)_2$ by XRD. On the basis of the details above, the formation of the present CRHA outer layer could be

mainly dependent on a procedure of dissolution (reaction (7)) and recrystallization (reaction (8)), accordingly, the elicited mechanism could be denominated as dissolution-recrystallization one.

In addition, the diffraction peak of $Al_2O_3 \cdot H_2O$ can also be found in Fig.8, which indicates the sealing of anodic Al_2O_3 pores caused by hydrothermal environment in autoclave[30].

3.4 Adhesive strength of composite coating

Using a mixture of epoxy resin and polyamide resin (1:1) as binder, it is tested that the adhesive strength of the HA/Al_2O_3 biocomposite coating formed at 2.0 mA/cm^2 on titanium is 9.5 MPa and then increases to 21.3 MPa, a value which could be compared to that of plasma-sprayed HA coatings on titanium[31], after hydrothermal treatment at 190 ℃ in autoclave.

It is reported that the adhesive strength between bioactive coatings and medical metal substrates could be improved by mechanically interlocking interface[32]. In this work, the mechanical interlocking may also be established due to the introduction of porous anodic Al_2O_3 intermediate layer which in-situ formed on PVD-deposited Al film on titanium. However, both the micrometric size of anodic Al_2O_3 pores and the interspace among electrodeposited CDHA crystals could weaken the enhancing effect for adhesion from mechanical interlocking. So, the hydrothermal treatment subsequent to electrodeposition is necessary for the HA/Al_2O_3 biocomposite coating on titanium to improve its adhesive strength and to enhance its biocompatibility. In other words, the narrowed pores and the nanometric network structure, which derive from the sealing of anodic Al_2O_3 pores and dissolution- recrystallization of HA coating as described in section 3.3, respectively, are beneficial for the adhesive strength of as-obtained biocomposite coating.

4 Conclusions

1) After anodization and chemical dissolution, anodic Al_2O_3 layer with uniform pores of approximately 1μm diameter forms on titanium. The XRD and EDS results show that Ca-deficient HA (CDHA) coatings are electrodeposited onto anodic Al_2O_3 on titanium due to the incorporation of HPO_4 group into the lattice of HA crystal. It is proposed that a potential dissolution-recrystallization procedure may lead to the conversion of CDHA coatings into Ca-rich HA(CRHA) ones during hydrothermal treatment. Tensile test results suggest that adhesive strength of the fabricated hydroxyapatite/Al_2O_3 biocomposite coating on titanium could be enhanced through a tighter interlocking between HA and anodic Al_2O_3 caused by hydrothermal treatment.

2) It is expected that the sandwich-like structure of hydroxyapatite/Al_2O_3/Ti obtained in the present work would result in a combination of superior biocompatibility with good mechanical properties and thus would provide a new choice for the surface biological modification of clinical hard tissue implants.

References

[1] HENCH L L. Bioceramics:from concept to clinic[J]. J Am Ceram Soc, 1991, 74: 1485−1510.

[2] KIM H M. Bioactive ceramics: challenges and perspectives[J]. J Ceram Soc Jpn, 2001, 109: S49−57.

[3] POSNER A S. The mineral of bone[J]. Clin Orthop Relat Res, 1985, 200: 87−89.

[4] AOKI H. Science and Medical Applications of Hydroxyapatite[M]. Tokyo: JAAS Press, 1991.

[5] KUMAR R R, WANG M. Functionally graded bioactive coatings of hydroxyapatite/titanium oxide composite system[J]. Materials Letters, 2002, 55: 133-137.

[6] REIS R L, MENTEIRO F J, HANSTINGS G W. Stability of hydroxylapatite plasma-sprayed coated Ti-6Al-4V under cyclic bending in simulated physiological solutions[J]. J Mater Sci Mater in Med, 1995, 6: 90−93.

[7] ANTONOV E N, BAGRATASHVILI V N, POPOV V K. Atomic force microscopic study of the surface morphology of apatite films deposited by pulsed laser ablation[J]. Biomaterials, 1997, 18: 1043−1049.

[8] LIU D M, YANG Q, TROCZYNSKI T. Sol-gel hydroxyapatite coatings on stainless steel substrates[J]. Biomaterials, 2002, 23: 691−698.

[9] LIN F H, HSU Y S, LIN S H. The effect of Ca/P concentration and temperature of simulated body fluid on the growth of hydroxyapatite coating on alkaline-treated 316L stainless steel[J]. Biomaterials, 2002, 23: 4029−4038.

[10] SHIRKHANZADEH M. Bioactive calcium phosphate coatings prepared by electrodeposition[J]. J Mater Sci Lett, 1991, 10: 1415−1417.

[11] ZHITOMIRSKY I, GALOR L. Electrophoretic deposition of hydroxyapatite[J]. J Mater Sci Mater in Med, 1997, 8: 213−219.

[12] BROWN S R, TURNER I G, REITER H. Residual stress measurement in thermal sprayed hydroxyapatite coating[J]. J Mater Sci, 1994, 5: 756−759.

[13] FATHI M , SALEHI M, SAATCHI A. In vitro corrosion behavior of bioceramic, metallic, and bioceramic-metallic coated stainless steel dental implants[J]. Dental Materials, 2003, 19: 188−198.

[14] ISHIZAWA H, OGINO M. Formation and characterization of anodic titanium oxide films containing Ca and P[J]. J Biomed Mater Res, 1995, 29: 65−72.

[15] ISHIZAWA H, OGINO M. Characterization of thin hydroxyapatite layers formed on anodic titanium oxide films containing Ca and P by hydrothermal treatment[J]. J Biomed Mater Res, 1995, 29: 1071−1079.

[16] HE Li-ping, WU Zhen-jun, CHEN Zong-zhang. In-situ growth of nanometric network calcium phosphate/porous Al_2O_3 biocomposite coating on Al-Ti substrate[J]. The Chinese Journal of Nonferrous Metals, 2004, 14(3): 460−464.(in Chinese)

[17] HE L P, MAI Y W, CHEN Z Z. Effects of anodization voltage on CaP/Al_2O_3-Ti nanometer biocomposites[J]. Nanotechnology, 2004, 15: 1465−1471.

[18] PATERMARAKIS G, MOUSSOUTZANIS K. Formulation of a criterion predicting the development of uniform regular and

non-uniform abnormal porous anodic alumina coatings and revealing the mechanisms of their appearance and progress[J]. Corrosion Science, 2001, 43: 1433−1464.

[19] THOMPSON G E. Porous anodic alumina: fabrication, characterization and applications[J]. Thin Solid Films, 1997, 297: 192−201.

[20] MARINO C E, OLIVEIRA E M, ROCHAFILHO R C. On the stability of thin-anodic-oxide films of titanium in acid phosphoric media[J]. Corrosion Science, 2001, 43: 1465−1476.

[21] WU Zhen-jun, HE Li-ping, CHEN Zong-zhang. Morphology and indirect inductive ability for calcium phosphate coatings of porous aluminum oxide synthesized in different electrolytes[J]. J Chinese Ceram Soc, 2004, 32: 1178−1183.(in Chinese)

[22] CHU S Z, WADA K, INOUE S. Synthesis and characterization of titania nanostructures on glass by Al anodization and sol-gel process[J]. Chem Mater, 2002, 14: 266−272.

[23] SHIRKHANZADEH M. Direct formation of nanophase hydroxyapatite on cathodically polarized electrodes[J]. J Mater Sci Mater in Med, 1998, 9: 67−72.

[24] HIDEKI M. Electrochemical deposition of calcium deficient apatite on stainless steel substrate[J]. J Ceram Soc Jpn, 1993, 101: 737−739.

[25] LIOU S C, CHEN S Y, LEE H Y. Structural characterization of nano-sized calcium deficient apatite powders[J]. Biomaterials, 2004, 25: 189−196.

[26] HAN Y, XU K W. Morphology and composition of hydroxyapatite coatings prepared by hydrothermal treatment on electrodeposited brushite coatings[J]. J Mater Sci Mater in Med, 1999, 10: 243−248.

[27] YEN S K, LIN C M. Cathodic reactions of electrolytic hydroxyapatite coating on pure titanium[J]. Mater Chem and Phy, 2003, 77: 70−76.

[28] CHU S Z, WADA K, INOUE S. Fabrication of TiO_2-$Ru(O_2)$/Al_2O_3 composite nanostructures on glass by Al anodization and electrodeposition[J]. J Electrochem Soc, 2004, 151: C38−44.

[29] KIM H M, HIMENO T, KOKUBO T. Process and kinetics of bonelike apatite formation on sintered hydroxyapatite in a simulated body fluid[J]. Biomaterials, 2005, 26: 4366−4373.

[30] LING H. Sealing: Enhance Anodic Coatings' Performance[M]. Technical Reports of METALAST© International Inc., 2001.

[31] WHITEHEAD R Y, LACEFIELD W R, LUCAS L C. Structure and integrity of a plasma sprayed hydroxyapatite coating on titanium[J]. J Biomed Mater Res, 1993, 27: 1501−1507.

[32] Tucker C. Deposition Technologies for Films and Coatings[M]. Park Ridge: Noyes Publications, 1982.

(Edited by LONG Huai-zhong)